

Performance of a high-current metal vapor vacuum arc ion source

Hiroshi Shiraishi

Nippon Steel Corporation, 46-59 Nakabaru, Tobata-ku, Kitakyusyu-city 804, Japan

Ian G. Brown

Lawrence Berkeley Laboratory, University of California, Berkley, California 94720

(Received 23 April 1990; accepted for publication 20 August 1990)

The operational characteristics of a metal vapor vacuum arc ion source have been studied. The beam current has been measured as a function of ion source extraction voltage (5–80 kV), arc current (50–250 A), metal-ion species (Ti, Ta, and Pb), and extractor grid spacing (0.89 and 0.38 cm). The measured beam current ranged up to 700 mA. The parametric variation of beam current is compared to that expected from the Child–Langmuir equation and excellent agreement is found.

I. INTRODUCTION

The metal vapor vacuum arc is a plasma discharge that occurs between metallic electrodes in vacuum^{1–4} and can be used within a high-current metal-ion source. This kind of source neither requires nor produces a gaseous ambient for its operation, and the bulk cathode material remains near room temperature; it is only at the micrometer-sized cathode spots that the solid metal of the cathode material is vaporized and ionized. The vacuum arc is an electrically efficient process, and a metal-ion plasma current of magnitude approximately 10% of the arc current is produced.⁵ Thus an ion source using the vacuum arc as the plasma formation mechanism is also an electrically efficient means of producing a high-current beam of metal ions.

Ion sources incorporating the vacuum arc as the plasma production mechanism have been investigated by several authors.^{6–15} The metal vapor vacuum arc (MEVVA) ion source developed at Lawrence Berkeley Laboratory was initially made for the injection of high-current beams of metal ions into the Bevalac heavy-ion synchrotron for basic nuclear physics research,^{16,17} more recently the source has also been used for high-dose metal-ion implantation for purposes including the formation of buried-metal silicide layers¹⁸ and the compositional fine tuning of high- T_c superconducting thin films.¹⁹ Several different embodiments of the MEVVA ion source have been designed and their performance has been reported on for isolated parameter regimes.^{6,15,20–22} In the work described here, we have studied the operational characteristics of the MEVVA IV ion source over a wide range of parameter space and compared the results with available theory. The metal-ion-beam current has been measured as a function of arc current, extractor voltage, metal species, extractor grid spacing, and position of the beam-current-measuring Faraday cup. The results illustrate the performance that can be obtained, and might serve to suggest new applications of this kind of high-current metal-ion source.

II. EXPERIMENTAL SETUP

In the MEVVA ion source, the intense plume of highly ionized metal plasma that is created at the cathode spots of a

metal vapor vacuum arc discharge is used to provide the plasma feedstock from which the ion beam is extracted. The quasi-neutral plasma plumes away from the cathode toward the anode and persists for the duration of the arc current drive. The anode of the discharge is located on axis with respect to the cylindrical cathode and has a central hole through which a part of the plasma plume streams; it is this component of the plasma that forms the medium from which the ions are extracted. The plasma plume drifts through the post-anode region to the set of grids that comprise the extractor.

In this work we used the MEVVA IV ion source. The main distinguishing characteristic of this embodiment of the concept is the multiple cathode feature, by means of which one can switch between different cathode materials easily and swiftly. Up to 16 separate cathode materials can be installed. For the experiments reported on here, cathodes of Ti, Ta, and Pb were used. The beam formation electrodes ("extractor grids") were a quite conventional set of multi-aperture, accel-decel grids (i.e., three grids—plasma grid, suppressor grid, and ground grid) of thickness 0.076 cm and in the form of a circular array of 31 holes each of diameter 0.3 cm, with an array diameter of approximately 2 cm; the beamlet holes were not shaped but were of simple cylindrical geometry. The extractor gap (distance between plasma grid and suppressor grid) was set at either 0.89 or 0.38 cm. A photograph of the MEVVA IV ion source is shown in Fig. 1.

It is convenient to operate the source in a mode where the beam extraction voltage is applied dc, and the arc current is pulsed. Here the extraction voltage was varied from 5 to 80 kV. A voltage of about -3 kV was applied to the suppressor grid to impede electron backstreaming. The arc current was of magnitude 50–250 A, and was supplied from an *LC* pulse line of impedance 1.5 Ω and pulse length 250 μ s. For these experiments the pulse repetition rate was several pulses per second, although the source has been operated at up to 100 pps.

The source was located on a vacuum chamber with a base pressure of about 5×10^{-7} Torr. Magnetically suppressed Faraday cups were positioned within the vessel to monitor the ion-beam current. The first Faraday cup, FC1,

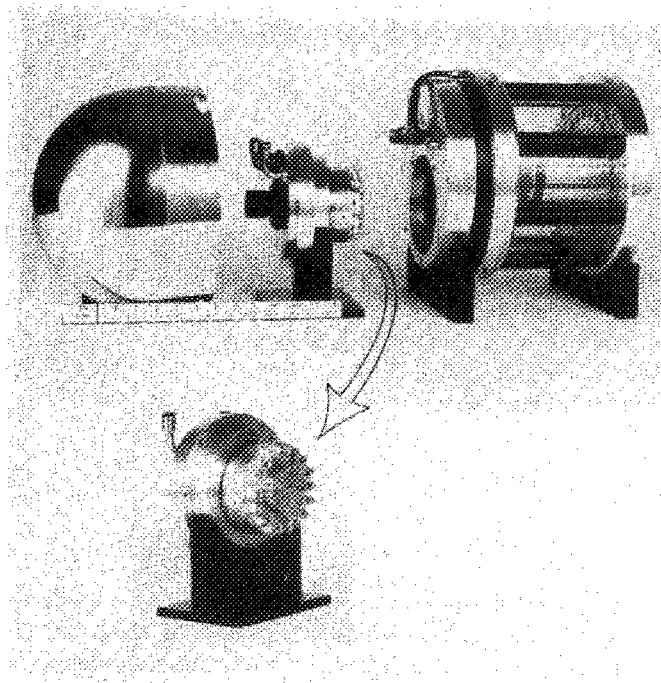


FIG. 1. Photograph of the MEVVA IV ion source showing the multiple cathode assembly.

had a rectangular entrance aperture of dimensions $7.3 \text{ cm} \times 15 \text{ cm}$, and was positioned at an axial distance of 20 cm from the ion-source extractor to the collector plate of the Faraday cup; this geometry is such that FC1 monitors essentially the entire beam produced (i.e., all the beam is collected). A second Faraday cup, FC2, was positioned at an axial distance of 59 cm from the source and could be used to monitor the beam current when FC1 was retracted. FC2 had a circular entrance aperture of 5 cm diam; this geometry is such that FC2 monitors only the beam current within a half-angle of approximately 2.5° . A schematic of the experimental configuration is shown in Fig. 2.

III. RESULTS

We measured the beam current, I_{beam} , using the two Faraday cups FC1 and FC2, as a function of extractor vol-

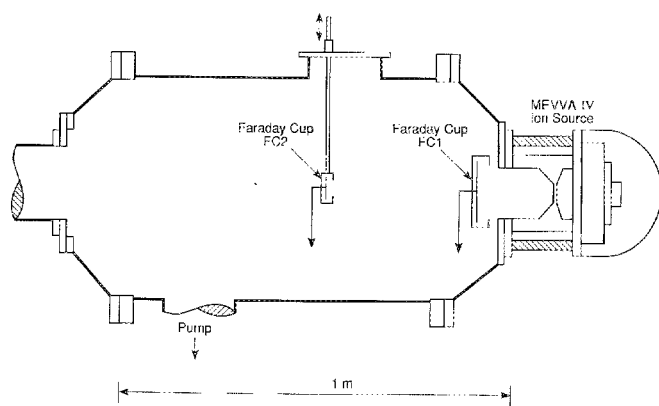


FIG. 2. Schematic of the experimental configuration.

tage V_{ext} and arc current I_{arc} , for the three different cathode materials Ti, Ta, and Pb, and for two different extractor grid spacings, $g = 0.89$ and 0.38 cm . The results are shown in Figs. 3–7.

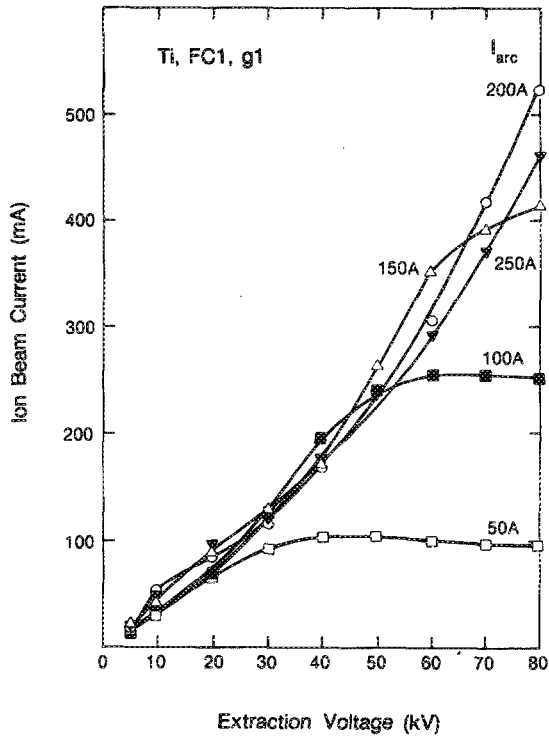
Beam current measured at the first Faraday cup FC1 as a function of extractor voltage is shown in Figs. 3(a)–3(c) for cathodes of Ti, Ta, and Pb, respectively, and for an extractor gap of 0.89 cm , where the arc current has been varied parametrically. One can see that: (1) the beam current generally increases with extractor voltage and arc current, and decreases with ion mass; (2) for a given arc current (vacuum arc plasma density) the beam current increases with extractor voltage up to a saturation value; (3) the saturation value is greater for higher arc current and for lower ion mass; and (4) for sufficiently high arc current the beam current no longer increases with arc current. These observations of the beam functional behavior are qualitatively as expected.

These data can be plotted as a function of arc current where the extractor voltage is varied as a parameter. The results are shown in Figs. 4(a)–4(c) for Ti, Ta, and Pb, respectively. The Ti data are particularly revealing in that an optimum extraction condition can clearly be seen, as indicated by the dashed line in Fig. 4(a); there is an arc current (i.e., plasma density) for which the beam current is a maximum for a given extraction voltage. In all these cases the beam current increases with extraction voltage for fixed arc current.

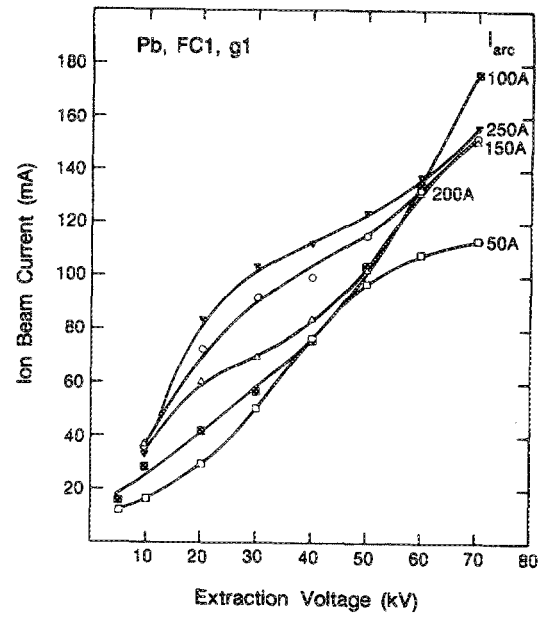
The beam current measured by Faraday cup FC2 is only a fraction of the total beam current. The half angle subtended by the 5-cm-diam cup at its distance of 59 cm from the ion source is 2.5° , implying a moderately “tight” ion beam. At an extraction voltage of 70 kV, for example, the corresponding normalized emittance of the beam monitored by FC2 lies in the approximate range $(5\text{--}10) \times 10^{-8} \pi \text{ m rad}$, depending on the particular metal-ion species employed. Thus the current measured at FC2 is a function of the beam emittance also, whereas that measured by FC1 is not. Figures 5(a)–5(c) show the beam current measured by FC2 as a function of arc current for Ti, Ta, and Pb, respectively, where the extraction voltage is varied parametrically. These curves are noticeably more peaked than for the corresponding FC1 curves, indicating that the variation of extraction optics and beam divergence as a function of arc current now plays an important role in the beam current collected. There is an optimum arc current at which the plasma density is best matched to the extraction optics.

The ratio of the beam current collected by FC2 to that collected by FC1 is plotted in Fig. 6 for the case of a Ta beam. The ratio $I_{\text{FC2}}/I_{\text{FC1}}$ has a maximum of 20% at optimum extraction parameters and falls to a low of about 8% over the range investigated. These data show clearly the effect of arc current and extraction voltage on the extraction optics and beam emittance, and indicate that a modest arc current of order 100–150 A provides the right conditions for optimum extraction optics.

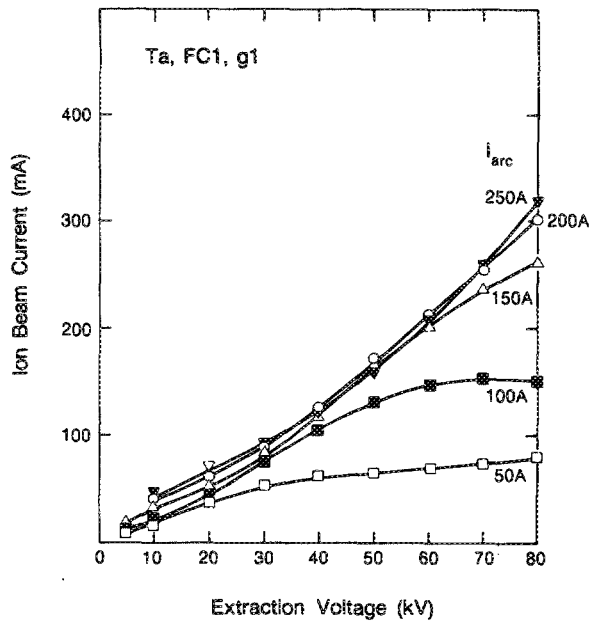
All of the above data were taken for a fixed ion-source extractor gap of $g = 0.89 \text{ cm}$. We reduced the gap width to $g = 0.38 \text{ cm}$ and the results of a limited data set are shown in Figs. 7(a)–7(c) for cathodes of Ti, Ta, and Pb, respectively.



(a)

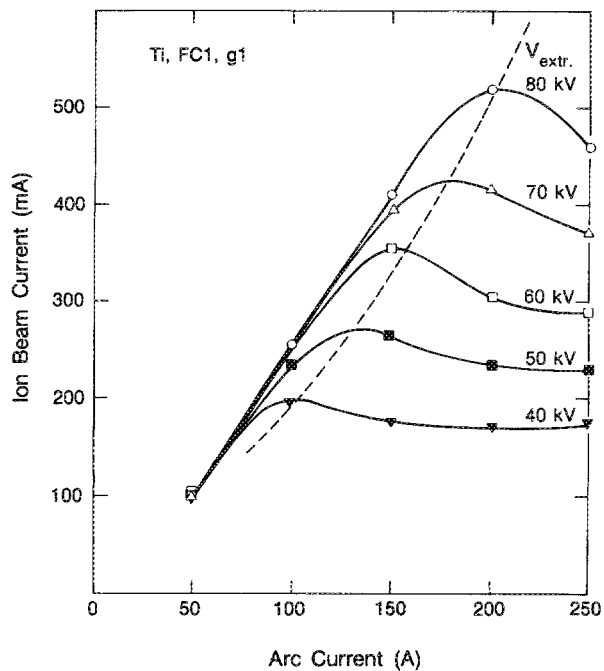


(c)

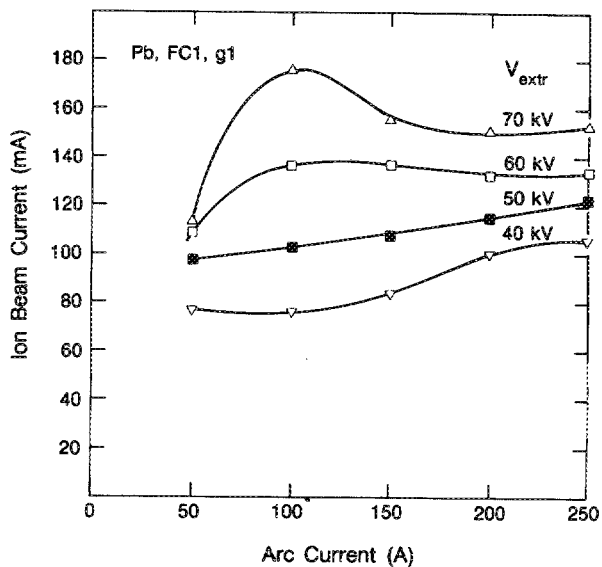


(b)

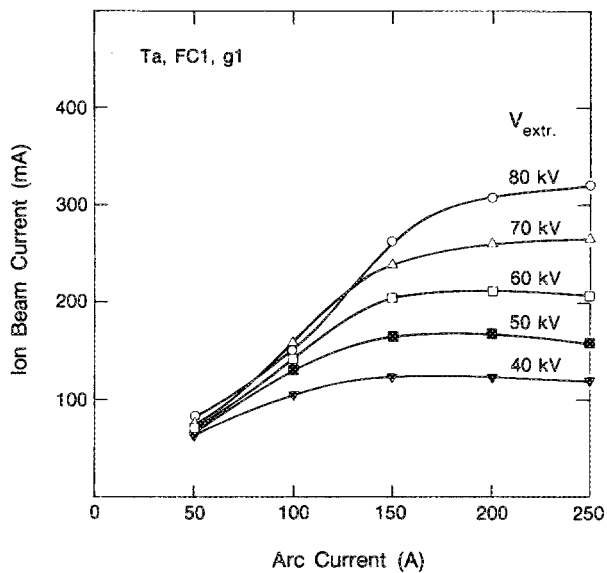
FIG. 3. Ion-beam current as a function of extraction voltage, with arc current as a parameter. Measured with FC1 and for an extraction gap $g = g_1 = 0.89$ cm. (a)Ti, (b)Ta, (c)Pb.



(a)

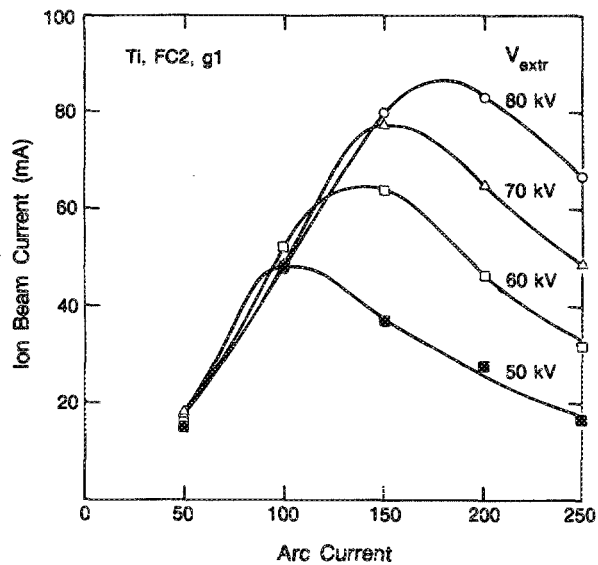


(c)

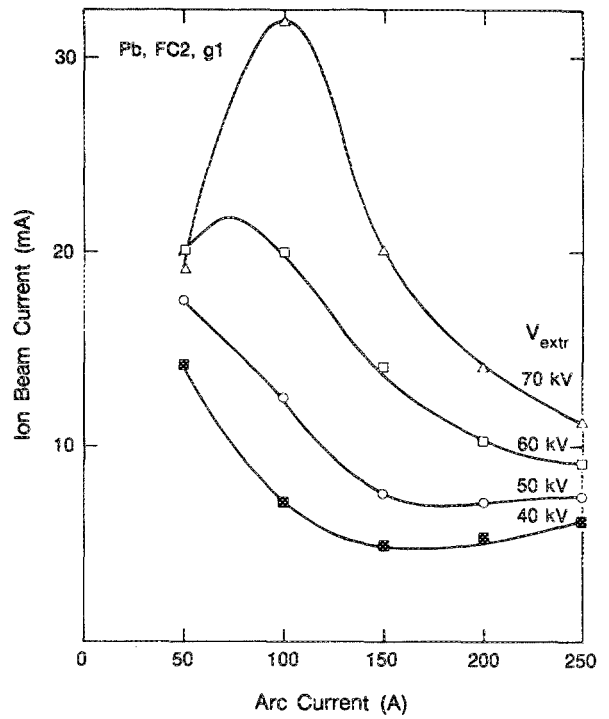


(b)

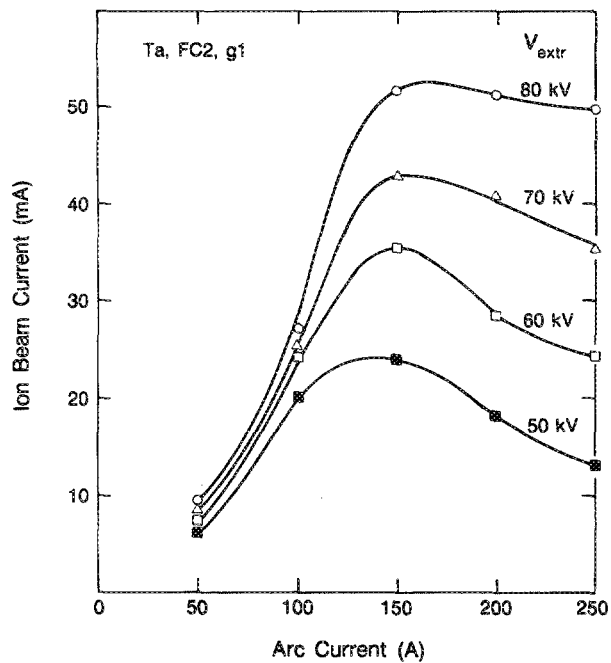
FIG. 4. Ion-beam current as a function of arc current, with extraction voltage as a parameter. Measured with FC1 and for an extraction gap $g = g_1 = 0.89$ cm. (a)Ti, (b)Ta, (c) Pb.



(a)



(c)



(b)

FIG. 5. Ion-beam current as a function of arc current, with extraction voltage as a parameter. Measured with FC2 and for an extraction gap $g = g_1 = 0.89$ cm. (a)Ti, (b)Ta, (c)Pb.

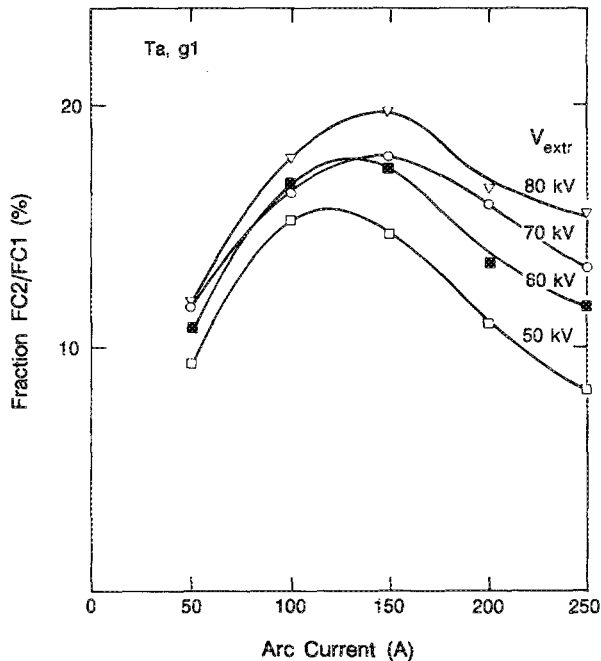


FIG. 6. Ratio of the ion-beam current measured by FC2 to that measured by FC1 as a function of arc current, with extraction voltage as a parameter. Extraction gap $g = g_1 = 0.89$ cm; Ti.

The beam current measured by the first Faraday cup FC1 is shown as a function of arc current, where the extraction voltage is varied parametrically. The beam current is greater than that obtained for the larger extractor spacing, as shown in Figs. 4(a)–4(c). An optimum arc current, at which the beam current is maximum for a given extractor voltage, is apparent in all cases.

IV. DISCUSSION

The current I that can be drawn from a plane, parallel geometry under space-charge-limited conditions is given by the Child–Langmuir equation^{23–25}

$$I = \frac{4}{9} \epsilon_0 S \left(\frac{2q_i}{M_i} \right)^{1/2} \frac{V^{3/2}}{d^2} = 1.72S \left(\frac{Q}{A} \right)^{1/2} \frac{V^{3/2}}{d^2}, \quad (1)$$

where S is the extractor (open) area, $q_i = eQ$ is the ion charge, $m_i = Am_{\text{amu}}$ is the ion mass, V the applied extraction voltage, d the extractor gap width, and in the second expression I is in mA, the voltage V is in kV, the area S in cm^2 , and the extractor gap d in cm. The validity of this simple form of the Child–Langmuir equation in providing a description of the ion current drawn between the plane, parallel electrodes of an ion source has been well confirmed by many authors over a wide range of parameters.^{24,25} It is thus of interest to compare the results obtained here with the Child–Langmuir predictions. Note that the beam is space

charge neutralized to a very high degree (except of course within the accelerating gap of the beam formation electrode system), as is demonstrated by the observation that the beam propagates without blowup¹⁴ (i.e., the beam trajectories are straight).

The variation of beam current with extractor voltage is shown in Fig. 8. The data for this comparison have been taken from Fig. 4(a) for Ti, Fig. 7(b) for Ta, and Fig. 7(c) for Pb. To best approximate the plane, parallel condition we have chosen those data that correspond to the optimal beam extraction conditions, in turn corresponding to the maxima that are visible in Figs. 4(a), 7(b), and 7(c). This optimum corresponds to the minimum beam divergence condition, and is also called the optimum perveance, or perveance match, condition. The straight lines drawn in Fig. 8 have a $V^{3/2}$ variation, and the excellent fit of the data to this predicted slope is evident.

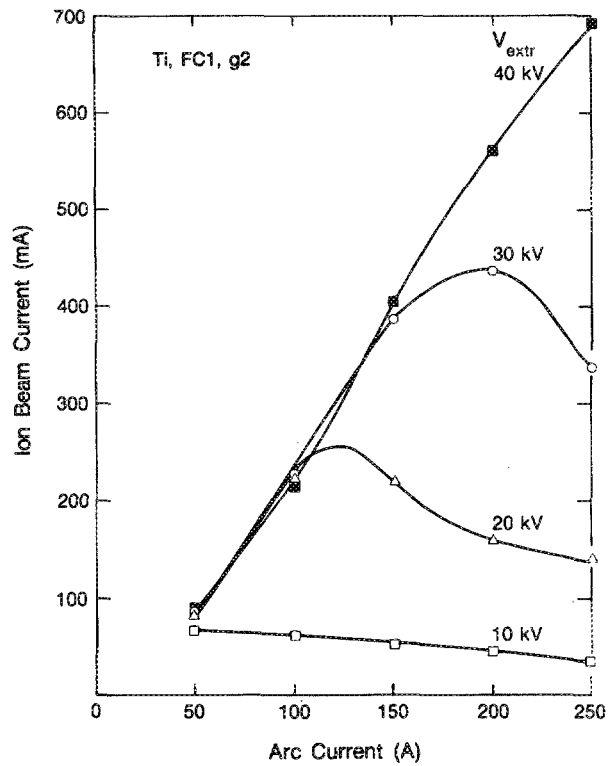
A comparison of the absolute values of the measured beam currents with the values predicted by the Child–Langmuir equation can be made also. The data shown in Fig. 8 can be used together with the \bar{Q} and A values listed in Table I and the geometric extraction area S given above to calculate theoretical beam currents for the cases of Ti, Ta, and Pb beams. The ratio I_m/I_{th} , where I_m is the measured beam current and I_{th} the theoretical value, for these three cases is 0.79, 0.48, and 0.49, respectively. We interpret this discrepancy (departure from unity) as due to the effective beam extraction area being less than the geometric value.

As a comparison of the variation of beam current with extractor gap, we take the effective gap width to be $d = g + r$, where g is the geometric separation and r is the hole radius. The Child–Langmuir prediction, $R_{\text{predicted}}$, for the ratio of the beam currents measured at two different extractor gaps is then simply $(d_1/d_2)^2$, or here ($g_1 = 0.89$ cm, $g_2 = 0.38$ cm, $r = 0.15$ cm), $R_{\text{predicted}} = 3.85$. Measured beam current ratios are 4.0 (Ti, 30 kV), 3.36 (Ta, 40 kV), and 2.74 (Pb, 40 kV), where again we have chosen the perveance match condition.

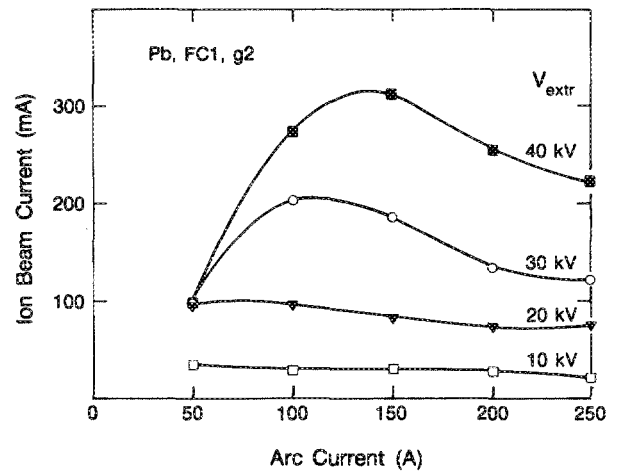
Finally, the variation of beam current with the charge-to-mass ratio, Q/A , of the beam species can be measured and compared with the Child–Langmuir prediction, and the results of this comparison are shown in Table I. Here the charge state Q has been taken as equal to the mean charge state \bar{Q} for the particular metal ion as measured in a series of

TABLE I. Beam current variation as a function of ion species charge-to-mass ratio: comparison of measured beam current ratios with that predicted from the Child–Langmuir equation. The predicted values ($R_{\text{predicted}}$) are determined from the $(\bar{Q}/A)^{1/2}$ ratios and the measured values (R_{measured}) from I_{beam} , the 60-kV data of Figs. 4(a)–4(c).

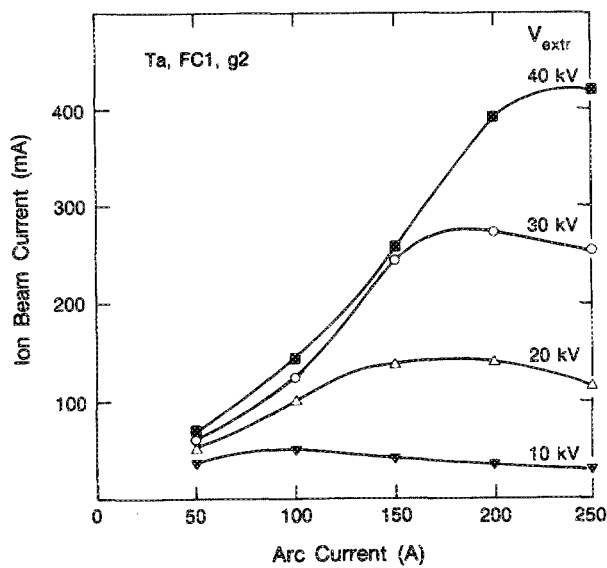
	Ti	Ta	Pb
\bar{Q}	2.14	2.96	1.53
A	48	181	207
$(\bar{Q}/A)^{1/2}$	0.211	0.128	0.086
I_{beam} (mA)	360	215	140
$R_{\text{predicted}}$	2.45	1.49	1
R_{measured}	2.57	1.54	1



(a)



(c)



(b)

FIG. 7. Ion-beam current as a function of arc current with extraction voltage as a parameter. Measured with FC1 and for an extraction gap $g = g_2 = 0.38$ cm. (a)Ti, (b)Ta, (c)Pb.

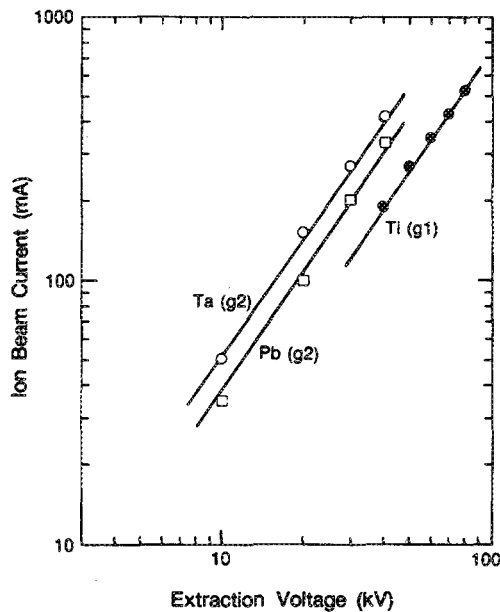


FIG. 8. Ion-beam current as a function of extraction voltage, with arc current adjusted for optimum beam extraction conditions. The straight lines are of slope $V^{3/2}$.

experiments previously made in our laboratory and reported elsewhere.^{6,26} The measured values of the beam current are maxima at 60 kV for g1 as shown in Figs. 4(a)–4(c) (i.e., perveance match for 60 kV with g1). The comparison of measured current ratios to predicted current ratios shows excellent agreement.

The beam current produced by the MEVVA IV ion source has been measured over a range of operating conditions as a function of the primary source parameters including extraction voltage, arc current, extraction gap, and metal-ion species. The variation of the beam current with extraction voltage, extraction gap, and charge-to-mass ratio of the ion species employed is in good agreement with that predicted by the Child–Langmuir equation. The metal-ion beam current varied up to a maximum of 700 mA over the range of parameters investigated here. These results demonstrate that the MEVVA ion source can be used to reliably produce intense pulsed metal-ion beams. A higher current version of metal vapor vacuum arc ion source is presently under development.

ACKNOWLEDGMENTS

We are indebted to Bob MacGill and Jim Galvin for their invaluable contributions to the design, fabrication, and

maintenance of the mechanical and electrical experimental facilities. This work was supported by the U. S. Army Research Office under Contract No. ARO 116-89, the Office of Naval Research under Contract No. N00014-88-F-0093, and the Department of Energy under Contract No. DE-AC03-76SF00098.

¹See, for instance, IEEE Trans. Plasma Sci. PS-11 (1983). Special issue on vacuum discharge plasmas.

²See, for instance, IEEE Trans. Plasma Sci. PS-13 (1985). Special issue on vacuum discharge plasmas.

³See, for instance, IEEE Trans. Plasma Sci. PS-15 (1987). Special issue on vacuum discharge plasmas.

⁴J. M. Lafferty, Ed., *Vacuum Arcs—Theory and Application* (Wiley, New York, 1980).

⁵C. W. Kimblin, J. Appl. Phys. 44, 3074 (1973).

⁶I. G. Brown, in *The Physics and Technology of Ion Sources*, edited by I. G. Brown (Wiley, New York, 1989), p. 331.

⁷R. K. Wakerling and A. Guthrie, Eds., *Electromagnetic Separation of Isotopes in Commercial Quantities* (McGraw-Hill, New York, 1951), p. 324.

⁸E. I. Revutskii, G. M. Skoromnyi, Yu. F. Kulygin, and I. I. Goncharenko, in *Proceedings of the Soviet Conference on Charged Particle Accelerators, Moscow, 9–16 October 1968*, edited by A. A. Vasilev, (published for the US AEC and NSF, Washington, DC, by the Israel Program for Scientific Translations), Vol. 1, p. 447.

⁹R. J. Adler and S. T. Picraux, Nucl. Instrum. Methods B 6, 123 (1985).

¹⁰S. Humphries, Jr., M. Savage, and D. M. Woodall, Appl. Phys. Lett. 47, 468 (1985).

¹¹C. Burkhart, S. Coffey, G. Cooper, S. Humphries, Jr., L. K. Len, A. D. Logan, M. Savage, and D. M. Woodall, Nucl. Instrum. Methods B 10, 792 (1985).

¹²I. G. Brown, J. E. Galvin, and R. A. MacGill, Appl. Phys. Lett. 47, 358 (1985).

¹³I. G. Brown, IEEE Trans. Nucl. Sci. NS-32, 1723 (1985).

¹⁴I. G. Brown, J. E. Galvin, B. F. Gavin, and R. A. MacGill, Rev. Sci. Instrum. 57, 1069 (1986).

¹⁵I. G. Brown, J. E. Galvin, R. A. MacGill, and R. T. Wright, *1987 Particle Accelerator Conference*, Washington, D.C., March, 1987, IEEE Catalog No. 87CH2387-9 (IEEE, New York, 1987), p. 343.

¹⁶J. R. Alonso, Nucl. Instrum. Methods A 244, 262 (1986).

¹⁷B. Feinberg and I. G. Brown, *1987 Particle Accelerator Conference*, Washington, D.C., March, 1987, IEEE Catalog No. 87CH2387-9 (IEEE, New York, 1987), p. 860.

¹⁸K. M. Yu, B. Katz, I. C. Wu, and I. G. Brown, Mater. Res. Soc. Symp. Proc. 147, 229 (1989).

¹⁹M. Rubin, I. G. Brown, E. Yin, and D. Wruck, J. Appl. Phys. 66, 3940 (1989).

²⁰I. G. Brown, J. E. Galvin, R. A. MacGill, and F. J. Paoloni, International Conference on Ion Sources, Berkeley, CA, July 10–14, 1989; Rev. Sci. Instrum. 61, 577 (1990).

²¹R. A. MacGill, I. G. Brown, and J. E. Galvin, International Conference on Ion Sources, Berkeley, CA, July 10–14, 1989; Rev. Sci. Instrum. 61, 580 (1990).

²²H. Shiraishi and I. G. Brown, International Conference on Ion Sources, Berkeley, CA, July 10–14, 1989; Rev. Sci. Instrum. 61, 589 (1990).

²³I. Langmuir and K. T. Compton, Rev. Mod. Phys. 3, 251 (1931).

²⁴T. S. Green, IEEE Trans. Nucl. Sci. NS-23, 918 (1976).

²⁵See, for instance, A. T. Forrester, *Large Ion Beams* (Wiley, New York, 1988).

²⁶I. G. Brown, B. Feinberg, and J. E. Galvin, J. Appl. Phys. 63, 4889 (1988).